



BUCKLING TEMPERATURE ANALYSIS OF LAMINATED COMPOSITE PLATES WITH CIRCULAR AND SEMICIRCULAR HOLES

Savaş EVRAN^{1,*}

^{1*} Department of Machine and Metal Technologies, Vocational School of Çanakkale Technical Sciences, Çanakkale Onsekiz Mart University, Çanakkale, Turkey

ABSTRACT

This statistical and numerical study deals with buckling temperature behavior of laminated composite plates with central circular and semicircular holes. Numerical buckling temperature analyses were performed using finite element software ANSYS based on Taguchi L18 orthogonal array. The plates were designed from graphite/epoxy systems. Fiber orientation angles and cutout shapes of the plates were assumed to be the control factors. Analysis of signal-to-noise ratio was used in order to investigate of the effects of fiber orientation angles and cutout shapes on the critical buckling temperature of the plates. Also, analysis of variance was performed in order to see percentage contribution rates and significance levels of control factors.

Keywords: Laminated composite, Cutout, Buckling temperature, Ply orientation, FEA

1. INTRODUCTION

Laminated plates made of composite materials are widely used in different areas such as marine, aerospace, and automotive [1]. In addition, laminated composite structures is used to instead of traditional metal to decrease the weight in the some areas of air vehicles [2]. The different solutions of laminated composite plates were generally analyzed using finite element method [3]. There are many studies for thermal buckling behaviors in the literature. Cetkovic [4] investigated the thermal buckling characteristic of laminated plates made of composite materials according to layerwise displacement model. Lakshmi narayana et al. [5] evaluated the thermal buckling behavior of laminated plates made from composite material according to elliptical and circular cutout. Topal and Uzman [6] presented a study including the optimal design of laminated plates made of composite material based on disturbed temperature load. Huang and Tauchert [7] examined the buckling characteristic of moderately thick symmetric angle-ply laminates with clamped boundary conditions under uniform temperature loads. Thangaratnam et al. [8] determined the buckling behavior of composite laminates based on critical temperature. Chen and Chen [9] reported the thermal buckling behavior of laminated plates made of composite materials under temperature loads. Prabhu and Dhanaraj [10] studied the thermal buckling characteristic of laminated plated made of composite materials and also used the finite element method. Shariyat [1] analyzed the thermal buckling behavior of rectangular multilayered made from composite materials based on uniform temperature loads and also used the layerwise plate theory. Manickam et al. [11] evaluated the thermal buckling of variable stiffness laminated plates made of composite under temperature loads and also used finite element method. Chen and Chen [12] reported the thermal buckling analysis of laminated plates made from composite materials under temperature loads and also utilized the finite element method. Ounis et al. [13] reported the thermal buckling analysis of laminated plates made of composite materials according to uniform temperature distribution and also used finite element method. Ergun [14] analyzed the buckling behavior of laminated plates made of composite material experimentally and numerically according to temperature influences. As can be seen from this literature, there are several studies about thermal buckling analysis of laminated composite plates. In addition, there is a study with experimental and numerical buckling analysis of laminated composite

with central circular and semicircular holes [15]. It is seen from literature mentioned that there are many studies including buckling analysis using laminated composite plates. In this study, numerical and statistical buckling temperature behavior of laminated composite plates with central circular and semicircular holes was studied for the first mode under temperature load. Plates have different cutout shapes such as central circular and semicircular holes.

2. MATERIALS and METHODS

In present study, the square laminated plates made of graphite/epoxy systems were used. The material properties of graphite-reinforced composite was shown in Table 1.

Table 1. Material constants [16-18]

E_1	$E_2=E_3$	$G_{12}=G_{13}$	G_{23}	$\nu_{12}=\nu_{13}$	ν_{23}	α_1	$\alpha_2=\alpha_3$
155 GPa	8.07 GPa	4.55 GPa	3.25 GPa	0.22	0.373	$-0.07 \times 10^{-6} \text{C}^{-1}$	$30.1 \times 10^{-6} \text{C}^{-1}$

The laminated composite plates have eight plies. The planar dimension of the square laminated composite plates was 0.15 in meters and the thickness of each layer was taken to be 0.000125 in meters [16]. The cutout shapes were considered to be diameters with 0.03 in meter. The numerical analysis was conducted based on Taguchi L18 orthogonal design. The orthogonal design has three control factors. The ply orientations and cutout shapes were considered to be control factors. The first control factor consists of two levels and the other control factors include three levels. The control factors and levels were exhibited in Table 2.

Table 2. Control factors and levels

Control Factors	Symbol	Unit	Levels		
Cutout Shapes	A	mm	Circular Hole	Semicircular Hole	-
First Four Laminates	B	Degree	0	5	10
Last Four Laminates	C	Degree	15	20	25

As can be seen from Table 2, three different control factors were used. The first control factor was determined as circular and semicircular holes whereas second and third control factors were employed to be fiber orientation angles assumed to vary from 0 to 25 in degree. Analysis of signal to noise ratio was used to determine the optimum result according to “higher is better” quality characteristic. The statistical analysis was carried out using Minitab 15 software [19]. The quality characteristic was given in Equation 1 [20].

$$(S/N)_{HB} = -10. \log \left(n^{-1} \sum_{i=1}^n (y_i^2)^{-1} \right) \tag{1}$$

where, n is used to be the number of buckling temperature analyses for a trial and yi shows ith data examined.

3. FINITE ELEMENT ANALYSIS

Numerical buckling temperature analyses were carried out using finite element software ANSYS [21]. In the analysis, SHELL281 element type was used and this element includes 8-nodes structural shell for six degrees of freedom depending on each node: translations for the x, y, and z axes, and rotations for the x, y, and z-axes [22]. The problem was described to be 3-D. Degree of freedom was assumed to be UX, UY, UZ, ROTX, ROTY, and ROTZ. Thus left and right edges of the plates under temperature load have clamped and remaining edges free boundary conditions. Globally assembled matrix was used to

be symmetric. Block Lanczos was used to be extraction technique. In modelling, eight laminates were used. The first four laminates has same fiber orientation angles whereas the other four laminates has different ply orientation from the first four laminates. Fiber angles with 0^0 were assumed in the axial direction. The laminated composite plates with different cutout shapes and layer stacking in x axis direction were exhibited in Figure 1.

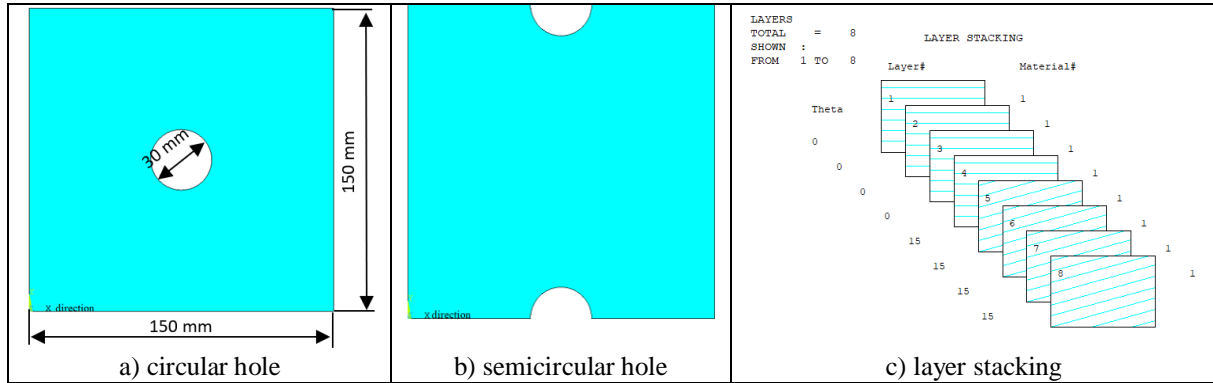


Figure 1. Cutout shapes and layer stacking of laminated composite plates.

4. RESULTS and DISCUSSIONS

In the study, thermal buckling behavior of laminated composite plates subjected to temperature load were analyzed using finite element method according to L18 orthogonal array. S/N ratio data based on numerical results were calculated using Minitab 15 statistical software according to “Larger is Better” quality characteristic. The critical buckling temperature and their S/N ratio values were tabulated in Table 3.

Table 3. Numerical results and S/N ratio values for L18 orthogonal array

Runs	Designation	Control Factors			Results	
		A	B	C	Temperature ΔT ($^{\circ}C$)	S/N ratio η (dB)
1	A ₁ B ₁ C ₁	CH	0	15	19.1964	25.6644
2	A ₁ B ₁ C ₂	CH	0	20	18.4583	25.3238
3	A ₁ B ₁ C ₃	CH	0	25	18.1662	25.1853
4	A ₁ B ₂ C ₁	CH	5	15	18.5235	25.3545
5	A ₁ B ₂ C ₂	CH	5	20	17.7732	24.9953
6	A ₁ B ₂ C ₃	CH	5	25	17.4460	24.8339
7	A ₁ B ₃ C ₁	CH	10	15	17.5092	24.8653
8	A ₁ B ₃ C ₂	CH	10	20	16.9144	24.5651
9	A ₁ B ₃ C ₃	CH	10	25	16.8966	24.5560
10	A ₂ B ₁ C ₁	SCH	0	15	18.9998	25.5750
11	A ₂ B ₁ C ₂	SCH	0	20	18.2387	25.2199
12	A ₂ B ₁ C ₃	SCH	0	25	17.9170	25.0653
13	A ₂ B ₂ C ₁	SCH	5	15	18.2587	25.2294
14	A ₂ B ₂ C ₂	SCH	5	20	17.4974	24.8595
15	A ₂ B ₂ C ₃	SCH	5	25	17.1528	24.6867
16	A ₂ B ₃ C ₁	SCH	10	15	17.1952	24.7081
17	A ₂ B ₃ C ₂	SCH	10	20	16.5998	24.4021
18	A ₂ B ₃ C ₃	SCH	10	25	16.5936	24.3988
Overall Mean ($\bar{\Delta T}$)					17.7409	-

Finite element results based on ANSYS software in Table 3 were demonstrated in Figure 2 visually. According to Figure 2, the least affected area of plates is monitored to be edges with clamped boundary conditions whereas the most affected area is determined to be the central region.

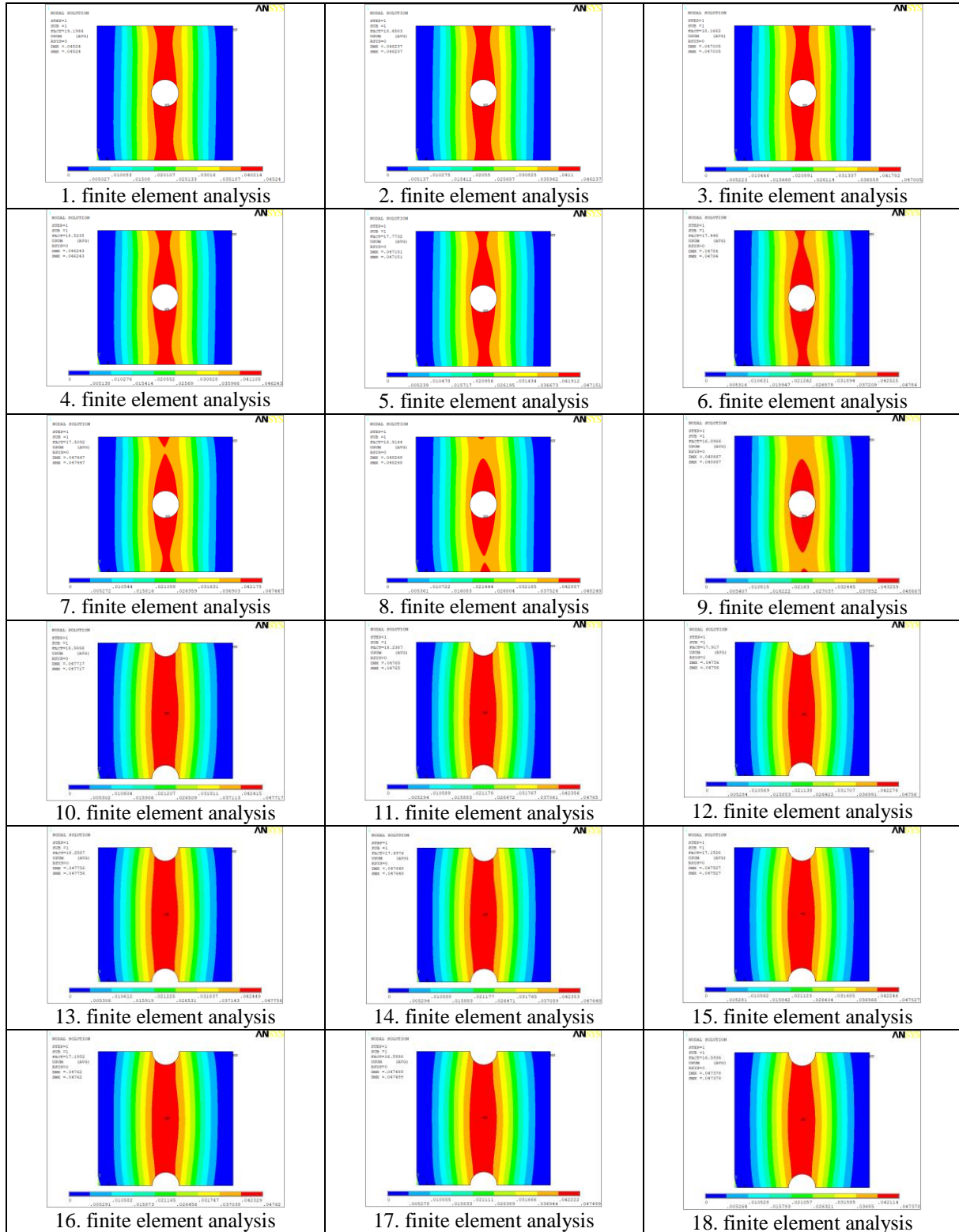


Figure 2. Finite element results based on L18 orthogonal array

4.1. Analysis of Optimal Levels

In order to determine the optimum levels of cutout shapes and fiber orientation angles on critical buckling temperature, numerical analyses were performed L18 orthogonal array based on Taguchi method. The average values of critical buckling temperatures for each control factor at all levels for numerical and S/N ratio data were calculated in order to select the optimum levels of control factors. These data were given in Table 4.

Table 4. Response table for S/N ratio and means data

Level	S/N ratio values in dB			Means in °C		
	A	B	C	A	B	C
1	25.04	25.34	25.23	17.88	18.50	18.28
2	24.90	24.99	24.89	17.61	17.78	17.58
3	-	24.58	24.79	-	16.95	17.36
Delta	0.13	0.76	0.45	0.27	1.54	0.92
Rank	3	1	2	3	1	2

According to Table 4, the optimum levels of cutout shapes and fiber orientation angles were determined to be level 1.

4.2. Analysis of Control Factors

In order to analyze the effect of each control factor, the average S/N ratio data calculated for control factors at all levels were used and these values were plotted in Figure 3.

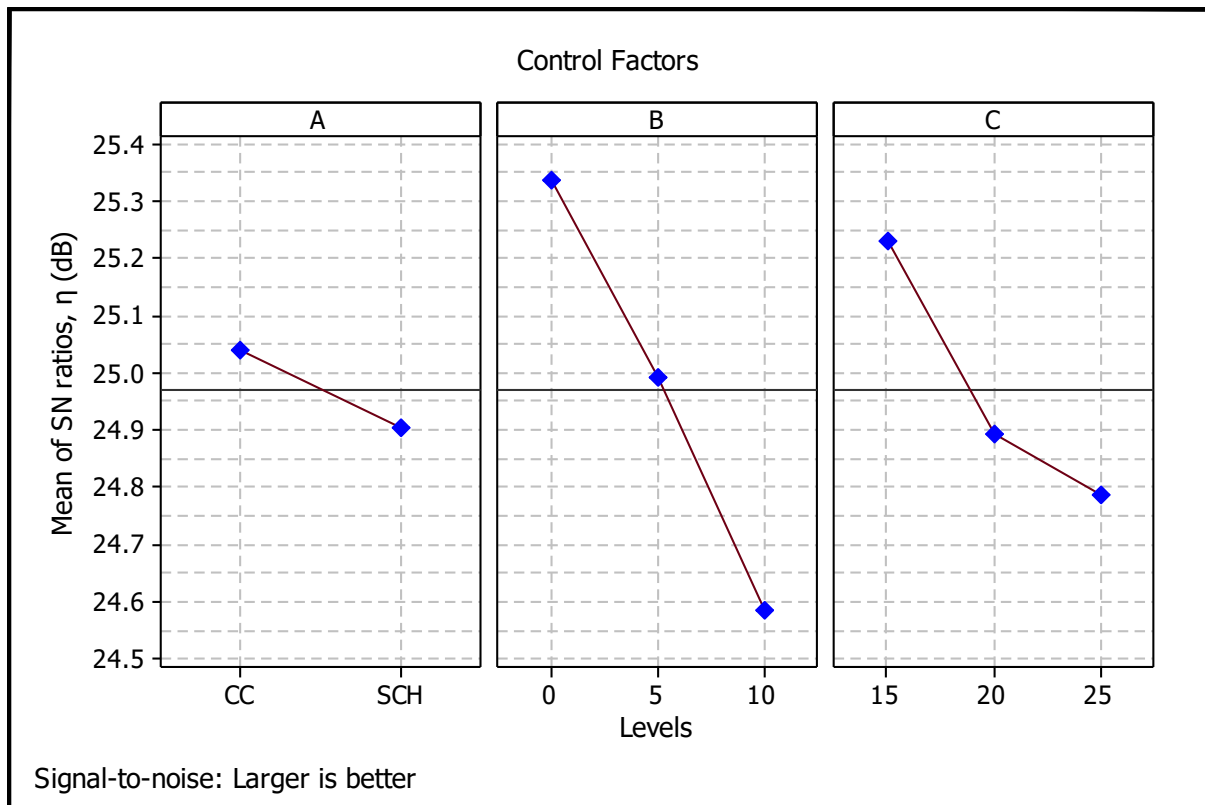


Figure 3. Effects of cutout shapes and fiber orientation angles

It can be seen from Figure 3 that buckling temperature of laminated composite plates with center circular holes is higher than plates with semicircular holes. In addition, increase of fiber orientation angles of the plates from 0 to 25 in degree provides the decrease of the critical buckling temperature values.

4.3. Analysis of Variance

Analysis of variance (ANOVA) was used in order to see the relationship between the dependent and independent control parameters. The significance levels of cutout shapes and fiber orientation angles and their percentage contributions on the critical buckling temperatures were calculated at 95% confidence level. The ANOVA results were exhibited in Table 5.

Table 5. ANOVA results for buckling temperature

Source	DF	Seq SS	Adj SS	Adj MS	F	P	% Contribution
A	1	0.3283	0.3283	0.3283	24.9000	0	3.15
B	2	7.1680	7.1680	3.5840	271.8500	0	68.81
C	2	2.7628	2.7628	1.3814	104.7800	0	26.52
Error	12	0.1582	0.1582	0.0132			1.52
Total	17	10.4172					100

It can be seen from ANOVA results that the strongest control parameters are obtained to be the first four laminates with 68.81 % effect, the second four laminated with 26.52 % effects, and cutout shape with 3.15 % effect respectively. Also, the cutout shapes and fiber orientation angles is significance control parameters on the buckling temperature of laminated composite plates since P values are lower than 0.05 data according to 95 % confidence level.

4.4. Analysis of Optimal Buckling Temperature

The optimal buckling temperature of the laminated composite plates along with the respective confidence intervals was estimated using significance control factors such as cutout and fiber orientation angles. The significance control factors were determined to be A1 with circular hole, B1 with fiber angle including 0°, and C1 with fiber angle which having 15°. The estimated mean of the critical buckling temperature for the first mode can be calculated as [20].

$$\text{Mean } \mu_\lambda = \bar{A}_1 + \bar{B}_1 + \bar{C}_1 - 2\bar{\Delta T} \tag{2}$$

According to Equation 2, $\bar{A}_1 = 17.88$, $\bar{B}_1 = 18.50$, and $\bar{C}_1 = 18.28$ were found to be the average data of critical first mode buckling temperature at the first level of the control factors in Table 4. In addition, the overall mean ($\bar{\Delta T}$) was calculated to be 17.7409 °C in Table 3. Substituting the values of varies terms in Equation 2, μ_λ is determined to be 19.1782 °C. The 95 % confidence intervals of confirmation finite element analysis and population were calculated based on Equation 3 and Equation 4 [20].

$$CI_{CA} = \left(F_{\alpha;1;n_2} V_{\text{error}} \left[\frac{1}{n_{\text{eff}}} + \frac{1}{R} \right] \right)^{1/2} \tag{3}$$

$$CI_{POP} = \left(\frac{F_{\alpha;1;n_2} V_{\text{error}}}{n_{\text{eff}}} \right)^{1/2} \tag{4}$$

$$n_{\text{eff}} = \frac{N}{(1 + T_{DOF})} \tag{5}$$

where, R is determined to be the sample size of confirmation finite element analyses and it is used to be 1. V_{error} is assumed to be the error data of variance in ANOVA results and it is solved to be 0.0132 value.

In addition, $\alpha = 0.05$ is used to be risk and $n_2 = 12$ is taken to be the error value according to the degree of freedom in ANOVA. $F_{0.05;1;12}$ is determined to be 4.75 [20] for F ratio data according to 95 % CI. In addition, N shows the total number of finite element analyses and it was determined to be 18 according to L18 orthogonal array. According to ANOVA, the total number of degrees of freedom based on the significance control factors is defined to be T_{DOF} and it is used to be 5. n_{eff} is calculated to be 6 thus CI_{CA} and CI_{POP} are calculated to be ± 0.2705 and ± 0.1022 respectively. The estimated confidence interval according to confirmation finite element analyses [20] is as follows:

$$\text{Mean } \mu_{\Delta T} - CI_{CA} < \mu_{\Delta T} < CI_{CA} + \text{Mean } \mu_{\Delta T}$$

The population according to the 95 % confidence interval [20] is as follows:

$$\text{Mean } \mu_{\Delta T} - CI_{POP} < \mu_{\Delta T} < CI_{POP} + \text{Mean } \mu_{\Delta T}$$

The predictive and numerical optimal results according to estimated confidence intervals were tabled in Table 6.

Table 6. Comparison of finite element and predictive results for 95 % confidence level

Optimal Designation	Numerical Result	Predicted Result	Estimated Confidence Intervals for 95% Confidence Level
A ₁ B ₁ C ₁	19.1964 °C	19.1782 °C	18.9077 < $\mu_{\Delta T}$ < 19.4487 for CI_{CA} 19.0760 < $\mu_{\Delta T}$ < 19.2804 for CI_{POP}

5. CONCLUSIONS

This numerical and statistical study is to analyze buckling temperature behavior of laminated composite plates. Fiber orientation angles of plates from 0 to 25 in degree were varied. The cutout shapes with central circular and semicircular holes, the first four, and the last four laminates were used as control factors. Finite element analyses were performed using ANSYS software and numerical design was conducted based on Taguchi’s L18 orthogonal array including three control factors. The first control factor has two levels and other control factors have three levels. Optimum levels of the control factors were determined using analysis of signal to noise (S/N) ratio. In addition, the levels of importance of control factors and percentage effects were analyzed using analysis of variance. According to present numerical and statistical study, the following conclusions can be summarized:

- Overall mean of numerical results for L18 orthogonal array was calculated to be 17.7409 °C.
- Buckling temperature of laminated composite plates with circular holes is higher than plates with semicircular holes.
- Increase of the fiber orientation angles from 0 to 25 in degree causes the decrease of the buckling temperature of laminated composite plates.
- Cutout shapes and fiber orientation angles are significance control factors on the buckling temperature because P value in ANOVA is smaller than 0.05 data at 95 % confidence level.
- On the thermal buckling behaviors, the least affected area of plates was analyzed to be edges with clamped boundary conditions whereas the most affected area was monitored to be the central region.
- The strongest control parameters are determined to be the first four laminates with 68.81 % effect, the second four laminated with 26.52 % effects, and cutout shape with 3.15 % effect respectively.
- Estimated buckling temperatures based on 95 % confidence intervals of confirmation analyses (CI_{CA}) and population (CI_{POP}) are found to be 18.9077 < μ_y < 19.4487 for CI_{CA} and 19.0760 < μ_y < 19.2804 for CI_{POP} respectively.

ACKNOWLEDGEMENTS

The research described in this paper was financially supported by the Research Fund of the Canakkale Onsekiz Mart University. Project Number: 3017.

REFERENCES

- [1] Shariyat M. Thermal buckling analysis of rectangular composite plates with temperature-dependent properties based on a layerwise theory. *Thin Walled Struct.* 2007; 45: 439-52.
- [2] Shiau L-C, Kuo S-Y, Chen C-Y. Thermal buckling behavior of composite laminated plates. *Compos. Struct.* 2010; 92: 508-14.
- [3] Zhang YX, Yang CH. Recent developments in finite element analysis for laminated composite plates. *Compos. Struct.* 2009; 88: 147-57.
- [4] Cetkovic M. Thermal buckling of laminated composite plates using layerwise displacement model. *Compos. Struct.* 2016; 142: 238-53.
- [5] Lakshmi narayana A, Vijaya Kumar R, Krishnamohana Rao G. Thermal buckling analysis of laminated composite plate with square/rectangular, elliptical/circular cutout. *Mater. Today: Proc.* 2018; 5: 5354-63.
- [6] Topal U, Uzman Ü. Thermal buckling load optimization of laminated composite plates. *Thin Walled Struct.* 2008; 46: 667-75.
- [7] Huang NN, Tauchert TR. Thermal buckling of clamped symmetric laminated plates. *Thin Walled Struct.* 1992; 13: 259-73.
- [8] Thangaratnam KR, Palaninathan, Ramachandran J. Thermal buckling of composite laminated plates. *Comput. Struct.* 1989; 32: 1117-24.
- [9] Chen LW, Chen LY. Thermal buckling of laminated composite plates. *J. Therm. Stresses* 1987; 10: 345-56.
- [10] Prabhu MR, Dhanaraj R. Thermal buckling of laminated composite plates. *Comput. Struct.* 1994; 53: 1193-204.
- [11] Manickam G, Bharath A, Das AN, Chandra A, Barua P. Thermal buckling behaviour of variable stiffness laminated composite plates. *Mater. Today Commun.* 2018; 16: 142-51.
- [12] Chen L-W, Chen L-Y. Thermal buckling behavior of laminated composite plates with temperature-dependent properties. *Compos. Struct.* 1989; 13: 275-87.
- [13] Ounis H, Tati A, Benchabane A. Thermal buckling behavior of laminated composite plates: a finite-element study. *Front. Mech. Eng.* 2014; 9: 41-9.
- [14] Ergun E. Experimental and numerical buckling analyses of laminated composite plates under temperature effects. *Adv Compos Lett* 2010; 19: 131-139.
- [15] Baba BO. Buckling behavior of laminated composite plates. *J. Reinf. Plast. Compos.* 2007; 26: 1637-55.
- [16] Meyers CA, Hyer MW. Thermal buckling and postbuckling of symmetrically laminated composite plates. *J. Therm. Stresses* 1991; 14: 519-40.

- [17] Meyers CA, Hyer MW. Thermally-induced, geometrically nonlinear response of symmetrically laminated composite plates. *Compos. Eng.* 1992; 2: 3-20.
- [18] Averill RC, Reddy JN. Thermomechanical postbuckling analysis of laminated composite shells. *Proceedings of the 34th AIAA/ASME/ASCE/AHS/ASC Structures, Structural Dynamics and Materials Conference: AIAA-93-1337-CP*; 1993. p. 351-60.
- [19] MINITAB. Software (Minitab Inc State College, PA, USA) (www.minitab.com).
- [20] Ross PJ. *Taguchi Techniques for Quality Engineering*: McGraw-Hill International Editions, 2nd Edition, New York, USA; 1996.
- [21] ANSYS. Software (ANSYS Inc, Canonsburg, PA, USA) (www.ansys.com).
- [22] ANSYS. Help (Version 13).